

Critical temperature for the two-dimensional attractive Hubbard model

Thereza Paiva,¹ Raimundo R. dos Santos,¹ R. T. Scalettar,² and P. J. H. Denteneer³

¹*Instituto de Física, Universidade Federal do Rio de Janeiro, Caixa Postal 68.528, 21945-970 Rio de Janeiro, Rio de Janeiro, Brazil*

²*Department of Physics, University of California, Davis, California 95616-8677, USA*

³*Instituut-Lorentz, Leiden University, P.O. Box 9506, 2300 RA Leiden, The Netherlands*

(Received 26 August 2003; revised manuscript received 19 February 2004; published 3 May 2004)

The critical temperature for the attractive Hubbard model on a square lattice is determined from the analysis of two independent quantities, the helicity modulus ρ_s and the pairing correlation function P_s . These quantities have been calculated through quantum Monte Carlo simulations for lattices up to 18×18 , and for several densities, in the intermediate-coupling regime. Imposing the universal-jump condition for an accurately calculated ρ_s , together with thorough finite-size scaling analyses (in the spirit of the phenomenological renormalization group) of P_s , suggests that T_c is considerably higher than hitherto assumed.

DOI: 10.1103/PhysRevB.69.184501

PACS number(s): 74.20.-z, 71.10.Pm, 74.25.Dw, 74.78.-w

The attractive Hubbard model^{1,2} has been successfully used to elucidate a number of important and fundamental issues in both conventional and high-temperature (cuprate) superconductivity. The nature of the crossover between BCS superconductivity (at weak coupling, or small on-site attraction) and Bose-Einstein condensation of tightly bound pairs (strong coupling) has been shown to be smooth.^{3,4} The appearance of preformed pairs within a certain range of parameters in the normal phase, especially below a characteristic temperature, has been related to pseudogap behavior of high-temperature superconductors.^{5,6} Further, this model allows one to introduce disorder on the fermionic degrees of freedom^{7,8} and investigate the behavior near the quantum critical point of the two-dimensional insulator-superconductor transition; this provides an alternative to the dirty-boson picture⁹ to discuss the universal conductivity.¹⁰ The attractive Hubbard model with a periodic modulation of U has been used to interpret superconductivity in layered structures.¹¹

A basic concern has run through many of these calculations, in particular, those based on quantum Monte Carlo (QMC) simulations. In two dimensions, there is a consensus that the early QMC phase diagram^{12,13}—in the space of critical temperature T_c , electronic density $\langle n \rangle$, and magnitude of the on-site attraction $|U|$ —is qualitatively correct. However, some serious quantitative discrepancies have emerged over the years, pointing towards higher critical temperatures; see, e.g., the Bogoliubov-Hartree-Fock (BHF) approach of Ref. 14. Our purpose here is to examine the dependence of T_c with $\langle n \rangle$, for fixed U , by resorting to a much wider (namely, larger system sizes and several electronic densities) set of QMC data, together with alternative procedures to locate the critical temperature. Establishing an accurate value for this most fundamental property of the model is important, especially as the physics of variants of the attractive Hubbard Hamiltonian is explored, and comparisons are made to the original system.

The model is defined by the Hamiltonian

$$\mathcal{H} = -t \sum_{\langle \mathbf{i}, \mathbf{j} \rangle, \sigma} (c_{\mathbf{i}\sigma}^\dagger c_{\mathbf{j}\sigma} + \text{H.c.}) - \mu \sum_{\mathbf{i}} (n_{\mathbf{i}\uparrow} + n_{\mathbf{i}\downarrow}) - |U| \times \sum_{\mathbf{i}} \left(n_{\mathbf{i}\uparrow} - \frac{1}{2} \right) \left(n_{\mathbf{i}\downarrow} - \frac{1}{2} \right), \quad (1)$$

where $c_{\mathbf{i}\sigma}$ ($c_{\mathbf{i}\sigma}^\dagger$) destroys (creates) an electron with spin σ on site \mathbf{i} of a square lattice, $\langle \mathbf{i}, \mathbf{j} \rangle$ denotes nearest-neighbor sites, $n_{\mathbf{i}\sigma} \equiv c_{\mathbf{i}\sigma}^\dagger c_{\mathbf{i}\sigma}$, $|U|$ is the strength of the attractive interaction, and μ is the chemical potential. From now on, all energies are expressed in units of the hopping amplitude t and we also set $k_B = 1$.

At half filling (which corresponds to the particle-hole symmetric point, $\mu = 0$), the degeneracy of charge-density wave (CDW) and singlet superconducting (SS) correlations leads to a three-component order parameter;¹⁵ the transition temperature is therefore suppressed to zero. Away from half filling, CDW correlations are suppressed and a finite-temperature Kosterlitz-Thouless (KT) transition¹⁶ into a SS phase takes place;^{13,17} this phase has only algebraically decaying correlations for $0 < T \leq T_c$. Further, close to half filling an exact mapping onto the two-dimensional Heisenberg antiferromagnetic model in a magnetic field leads to^{12,13} $T_c \approx -2\pi J / \ln|1 - \langle n \rangle|$, so that T_c rises sharply from zero as one dopes away from $\langle n \rangle = 1$.

We start by employing the analysis of Ref. 13 to new data for the SS pairing correlation function,

$$P_s = \langle \Delta^\dagger \Delta + \Delta \Delta^\dagger \rangle \quad (2)$$

with

$$\Delta^\dagger = \frac{1}{\sqrt{N}} \sum_{\mathbf{i}} c_{\mathbf{i}\uparrow}^\dagger c_{\mathbf{i}\downarrow}. \quad (3)$$

For $0 < T \leq T_c$, one expects

$$\Gamma(r) \equiv \langle c_{\mathbf{i}\uparrow}^\dagger c_{\mathbf{i}\downarrow}^\dagger c_{\mathbf{j}\downarrow} c_{\mathbf{j}\uparrow} + \text{H.c.} \rangle \sim r^{-\eta(T)}, \quad (4)$$

where $r \equiv |\mathbf{i} - \mathbf{j}|$, and $\eta(T)$ increases monotonically between $\eta(0) = 0$ and $\eta(T_c) = 1/4$.^{16,18}

The finite-size scaling behavior of P_s is therefore obtained upon integration of $\Gamma(r)$ over a two-dimensional system of linear dimension L . One then has¹³

$$P_s = L^{2 - \eta(T_c)} f(L/\xi), \quad L \gg 1, T \rightarrow T_c^+ \quad (5)$$

with

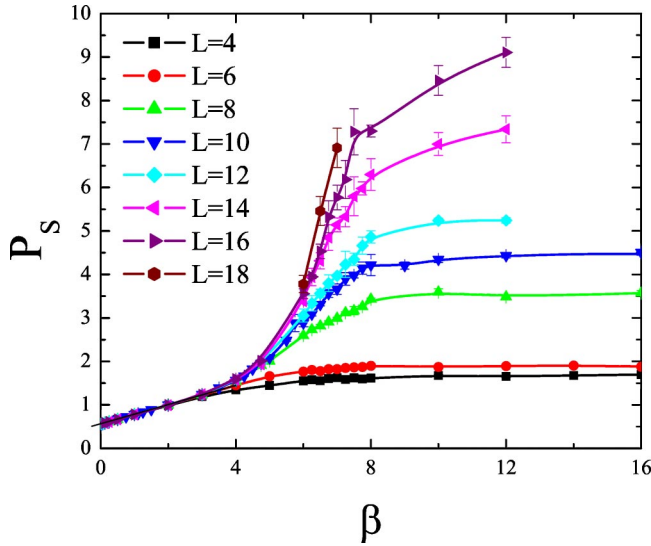


FIG. 1. (Color online) P_s as a function of $\beta \equiv 1/T$ for $\langle n \rangle = 0.5$ and different lattice sizes L .

$$\xi \sim \exp\left[\frac{A}{(T-T_c)^{1/2}}\right]; \quad (6)$$

in the thermodynamic limit, one recovers $P_s \sim \xi^{7/4}$. For completeness, one should mention that since $\eta \rightarrow 0$ as $T \rightarrow 0$, the system displays long-range order in the ground state, so that a “spin-wave scaling” is expected to hold,¹⁹

$$\frac{P_s}{L^2} = |\Delta_0|^2 + \frac{C}{L}, \quad (7)$$

where Δ_0 is the superconducting gap function at zero temperature, and C is a $|U|$ -dependent constant.

Similarly to Ref. 13, here we use the determinant QMC algorithm²⁰ to calculate P_s . Typically our data have been obtained after 500 warming-up steps followed by 50 000 sweeps through the lattice. The discretized imaginary-time interval²⁰ was set to $\Delta\tau = 0.125$, which is small enough for the results not to depend on this choice in any significant way.

In Fig. 1 we show raw data for P_s as a function of $(1/T)$, for fixed density, $\langle n \rangle = 0.5$ and $U = -4$, and for different lattice sizes. The crossover between temperature- and size-limited regimes is described by finite-size scaling (FSS) theory²¹ and appears as a leveling off of P_s below a certain temperature for each system size. Before a more quantitative scaling analysis, we can already see a suggestion that T_c is around $1/6$ from the raw P_s data. In general, at temperatures for which correlations are short ranged, a structure factor like P_s is independent of lattice size. As T is decreased, the point at which the structure factor begins growing with lattice size signals the temperature at which the correlation length ξ is becoming large (comparable to the lattice size L), thus providing a crude estimate of T_c . The subsequent plateau at low temperatures occurs when $\xi \gg L$. This crossover is contemplated by the FSS form, Eq. (5), which can be invoked to determine T_c by plotting $L^{-7/4}P_s$ as a function of

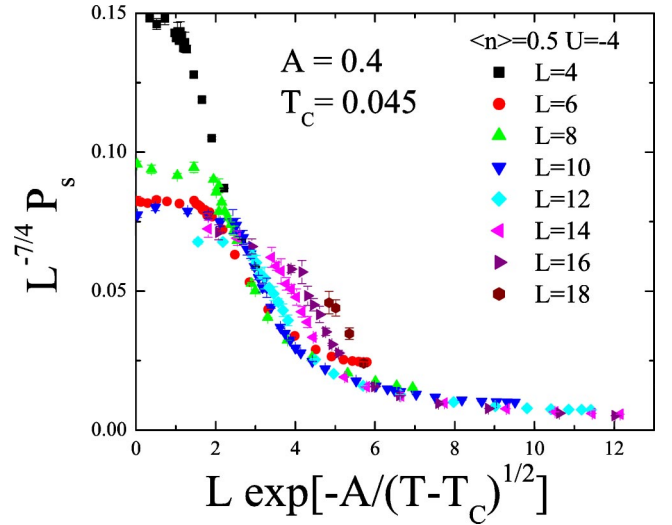


FIG. 2. (Color online) Rescaled P_s as a function of $w \equiv L \exp[-A/(T-T_c)^{1/2}]$ for $\langle n \rangle = 0.5$ and different lattice sizes L . The values for A and T_c are the ones determined in Ref. 13.

$w \equiv L \exp[-A/(T-T_c)^{1/2}]$, at a given U , for different system sizes, with T_c and A being adjusted to give the best possible data collapse, as done in Ref. 13. Figure 2 shows the resulting scaling plot, in which the values $A = 0.4$ and $T_c = 0.045$ were determined in Ref. 13. With our substantially increased amount of data points it becomes clear that the data collapse onto a single curve with the parameters A and T_c of Ref. 13 becomes rather unsatisfactory. We furthermore note that Eq. (6) is expected to hold only for $t \leq 10^{-2}$ [$t \equiv (T-T_c)/T_c$], see, e.g., Ref. 22. For the value of T_c used in Fig. 2, only few data obtained for $L = 4, 6, 8, 10$ in Ref. 13 satisfy this criterion.

We therefore obtain new values of A and T_c from our expanded data set. We disregard the data from the smallest system sizes, $L = 4$ (which, additionally, has a special topology, being equivalent to a $2 \times 2 \times 2 \times 2$ four-dimensional lattice), $L = 6$, $L = 8$, and also $L = 10$; as we will see below, the SS pairing correlation function presents large finite size effects for these lattice sizes. Furthermore, we only include data points for temperatures T for which Eq. (6) is expected to hold (see above). Figure 3 clearly shows that, for the larger lattices, our newly determined parameters $A = 0.1$ and critical temperature $T_c = 0.13$ render a much better data collapse than the old parameters.

The present analysis shows that the estimates of T_c obtained in Ref. 13 can be quantitatively quite unreliable. In our opinion, this is due to the fact that the finite-size behavior of P_s , Eqs. (5) and (6), follows from an analysis which is valid only for large enough lattice sizes, since it involves the binding-unbinding of rather large structures (vortices) in the KT transition.¹⁶ Moreover, the parameters A and T_c that have to be found via data fitting both reside in an exponent, resulting in large uncertainties for the individual fitted parameters. Although the lattice sizes used in the present study may not be large enough to determine T_c with high accuracy, our result is bound to be an improvement and in any case indicates that the actual T_c may be much larger (by even a factor of 3) than believed so far.

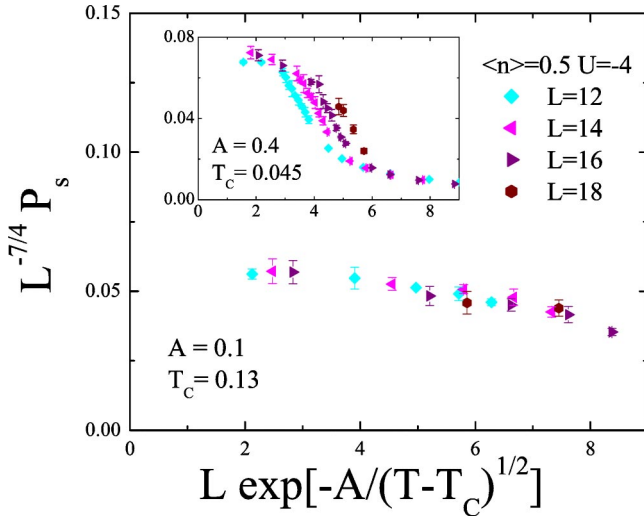


FIG. 3. (Color online) Same as Fig. 2, but with A and T_c determined from the present data. Inset shows same system sizes, with A and T_c from Ref. 13.

This tendency towards higher critical temperatures appears as well in a completely independent analysis, based on the behavior of the helicity modulus (HM). The latter is a measure of the response of the system in the ordered phase to a “twist” of the order parameter,²³ and can be expressed in terms of the current-current correlation functions as follows.²⁴

$$\rho_s = \frac{D_s}{4\pi e^2} = \frac{1}{4} [\Lambda^L - \Lambda^T], \quad (8)$$

where D_s is the superfluid weight, and

$$\Lambda^L \equiv \lim_{q_x \rightarrow 0} \Lambda_{xx}(q_x, q_y=0, \omega_n=0) \quad (9)$$

and

$$\Lambda^T \equiv \lim_{q_y \rightarrow 0} \Lambda_{xx}(q_x=0, q_y, \omega_n=0) \quad (10)$$

are, respectively, the limiting longitudinal and transverse responses, with

$$\Lambda_{xx}(\vec{q}, \omega_n) = \sum_{\vec{\ell}} \int_0^\beta d\tau e^{i\vec{q}\cdot\vec{\ell}} e^{i\omega_n\tau} \Lambda_{xx}(\vec{\ell}, \tau), \quad (11)$$

where $\omega_n = 2n\pi T$,

$$\Lambda_{xx}(\vec{\ell}, \tau) = \langle j_x(\vec{\ell}, \tau) j_x(0, 0) \rangle, \quad (12)$$

where

$$j_x(\vec{\ell}, \tau) = e^{\mathcal{H}\tau} \left[it \sum_{\sigma} (c_{\vec{\ell}+\hat{x},\sigma}^\dagger c_{\vec{\ell},\sigma} - c_{\vec{\ell},\sigma}^\dagger c_{\vec{\ell}+\hat{x},\sigma}) \right] e^{-\mathcal{H}\tau} \quad (13)$$

is the x component of the current density operator; see Ref. 24 for details.

At the KT transition, the following universal-jump relation involving the helicity modulus holds:²⁵

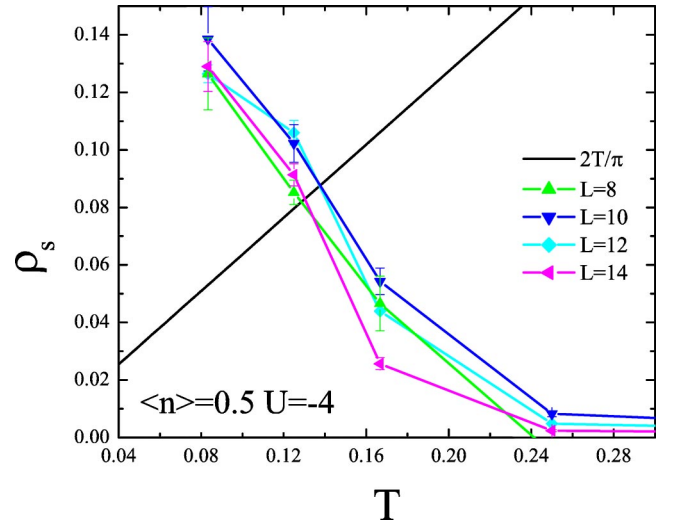


FIG. 4. (Color online) Helicity modulus as a function of temperature for $\langle n \rangle = 0.5$ and different lattice sizes L . The straight line corresponds to $2T/\pi$.

$$T_c = \frac{\pi}{2} \rho_s^-, \quad (14)$$

where ρ_s^- is the value of the helicity modulus just below the critical temperature. Thus we can obtain T_c by plotting $\rho_s(T)$, and looking for the intercept with $2T/\pi$. This procedure has been used before, with ρ_s calculated within a BHF approximation,^{14,26} since transverse current-current correlations were neglected, ρ_s is likely to have been overestimated, and the ensuing T_c 's may have been too high. Here we calculate both Λ^L and Λ^T by QMC simulations to obtain ρ_s through Eq. (8); a typical example of $\rho_s(T)$, for $\langle n \rangle = 0.5$, is shown in Fig. 4. We see that finite-size effects are not too drastic, since all curves cross the straight line within a small range of temperatures; that is, from Fig. 4 we can estimate $T_c = 0.14 \pm 0.02$.

In order to check the robustness of this method, we can extract T_c from P_s through a “phenomenological renormalization group” (PRG) (Refs. 27 and 28) analysis, provided some subtleties peculiar to the KT transition are kept in mind. Since $\xi \rightarrow \infty$ for all $T < T_c$, Eq. (5) implies that curves for $L^{-7/4} P_s(L, \beta)$, when plotted as functions of β , and for different L , should all *merge* for $\beta > \beta_c$. Figure 5 shows that this characteristic feature only sets in for the largest system sizes, namely, $L \geq 12$, from which we can infer $\beta_c = 7.5 \pm 0.25$; these error bars are somewhat arbitrary, and result from visual inspection. It should be stressed that this estimate for β_c agrees remarkably well with the one obtained from the helicity modulus, indicating the robustness of both procedures to extract T_c . Interestingly, we should notice that the curves for $L=6$ and 8 *cross* each other (as in an ordinary second-order transition) at $\beta \approx 7$, which is very close to β_c estimated from the larger systems. Therefore, within the context of PRG, for the smallest sizes a KT transition appears as an ordinary transition, only crossing over to the merging feature for the largest sizes.

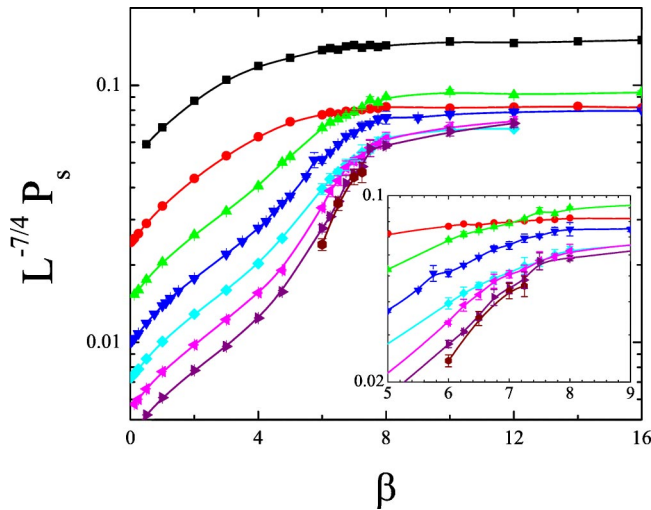


FIG. 5. (Color online) Logarithm-linear plot for the rescaled P_s as a function of β , for $\langle n \rangle = 0.5$ and for different lattice sizes L , symbols are the same as in Fig. 2. The inset shows a blowup of the region centered about $\beta = 7$. No parameters are adjusted.

The critical temperature has been estimated for other electronic densities, $\langle n \rangle = 0.1$ (HM and PRG), 0.3 (PRG), 0.7 (PRG), and 0.875 (HM and PRG); all PRG plots display the crossing and merging tendency observed for $\langle n \rangle = 0.5$. The resulting phase diagram is shown in Fig. 6; for comparison, we also plot the early QMC results,¹³ the parquet data from Luo and Bickers,²⁹ and the estimates from the BHF approximation.¹⁴ While close to half filling all results (but BHF) are in fair agreement, for larger dopings agreement is only found between the results from PRG and those from the helicity modulus. The inescapable conclusion is that the critical temperature for the superconducting transition in the attractive Hubbard model is actually higher than previously assumed.

In summary, we have established very reliable estimates for the critical temperature of the square-lattice attractive

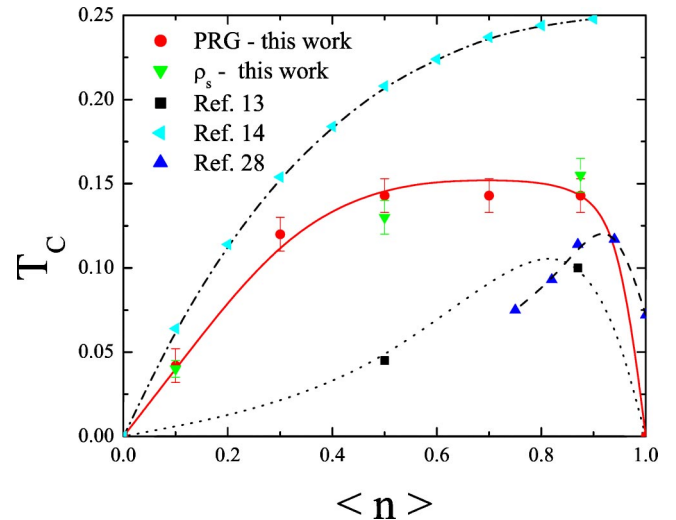


FIG. 6. (Color online) Critical temperature as a function of band filling, obtained by different methods. All lines through data points are guides to the eye.

Hubbard model. This is done by finding quantitative agreement between entirely different procedures to extract T_c from two independent correlation functions (both computed by determinant QMC). As a result, the critical temperature is found to be substantially higher than the currently accepted values, also obtained using QMC, but with a different data analysis; as expected, they are also substantially lower than estimates obtained within a Hartree-Fock/mean-field approximation.

The authors are grateful to S. de Queiroz and A. Moreo for discussions. T.P. and R.R.dS. acknowledge partial financial support by Brazilian Agencies FAPERJ, CNPq, Instituto do Milênio para Nanociências/MCT, and Rede Nacional de Nanociências/CNPq; R.T.S. acknowledges support by NSF-DMR-0312261. This research was further supported by a joint CNPq-690006/02-0/NSF-INT-0203837 grant.

¹R. Micnas, J. Ranninger, and S. Robaszkiewicz, *Rev. Mod. Phys.* **62**, 113 (1990).

²J.A. Wilson, *J. Phys.: Condens. Matter* **13**, R945 (2001).

³A.J. Leggett, in *Modern Trends in the Theory of Condensed Matter*, edited by A. Pekalski and J. Przystawa (Springer, Berlin, 1980).

⁴M. Randeria, in *Proceedings of the International School of Physics "Enrico Fermi,"* edited by G. Iadonisi, J.R. Schrieffer, and M. Chiofalo (IOS Press, Amsterdam, 1998).

⁵M. Randeria, N. Trivedi, A. Moreo, and R.T. Scalettar, *Phys. Rev. Lett.* **69**, 2001 (1992).

⁶R.R. dos Santos, *Phys. Rev. B* **50**, 635 (1994).

⁷G. Litak, K.I. Wysokiski, R. Micnas, and S. Robaszkiewicz, *Physica C* **199**, 191 (1992).

⁸R.T. Scalettar, N. Trivedi, and C. Huscroft, *Phys. Rev. B* **59**, 4364 (1999).

⁹M.P.A. Fisher, G. Grinstein, and S.M. Girvin, *Phys. Rev. Lett.* **64**,

587 (1990).

¹⁰S.-Y. Hsu, J.A. Chervenak, and J.M. Valles, Jr., *Phys. Rev. Lett.* **75**, 132 (1995).

¹¹T. Paiva, M. El Massalami, and R.R. dos Santos, *J. Phys.: Condens. Matter* **15**, 7917 (2003).

¹²R.T. Scalettar, E.Y. Loh, Jr., J.E. Gubernatis, A. Moreo, S.R. White, D.J. Scalapino, R.L. Sugar, and E. Dagotto, *Phys. Rev. Lett.* **62**, 1407 (1989).

¹³A. Moreo and D.J. Scalapino, *Phys. Rev. Lett.* **66**, 946 (1991).

¹⁴P.J.H. Denteneer, G. An, and J.M.J. van Leeuwen, *Europhys. Lett.* **16**, 5 (1991); *Phys. Rev. B* **47**, 6256 (1993).

¹⁵H. Shiba, *Prog. Theor. Phys.* **48**, 2171 (1972).

¹⁶J.M. Kosterlitz and D.J. Thouless, *J. Phys. C* **6**, 1181 (1973).

¹⁷F.F. Assaad, W. Hanke, and D.J. Scalapino, *Phys. Rev. B* **49**, 4327 (1994).

¹⁸B. Berche, A. Farinas Sanchez, and R. Paredes, *Europhys. Lett.* **60**, 539 (2002).

- ¹⁹D.A. Huse, Phys. Rev. B **37**, 2380 (1988).
- ²⁰R. Blankenbecler, R.L. Sugar, and D.J. Scalapino, Phys. Rev. D **24**, 2278 (1981); S.R. White, D.J. Scalapino, R.L. Sugar, E.Y. Loh, Jr., J.E. Gubernatis, and R.T. Scalettar, Phys. Rev. B **40**, 506 (1989); R.R. dos Santos, Braz. J. Phys. **33**, 36 (2003).
- ²¹J.L. Cardy, *Current Physics—Sources and Comments* (North-Holland, Amsterdam, 1988), Vol. 2.
- ²²R. Gupta and C.F. Baillie, Phys. Rev. B **45**, 2883 (1992).
- ²³M.E. Fisher, M.N. Barber, and D. Jasnow, Phys. Rev. A **8**, 1111 (1973).
- ²⁴D.J. Scalapino, S.R. White, and S.C. Zhang, Phys. Rev. Lett. **68**, 2830 (1992); Phys. Rev. B **47**, 7995 (1993).
- ²⁵D.R. Nelson and J.M. Kosterlitz, Phys. Rev. Lett. **39**, 1201 (1977).
- ²⁶P.J.H. Denteneer, Phys. Rev. B **49**, 6364 (1994).
- ²⁷M.P. Nightingale, J. Appl. Phys. **53**, 7927 (1982).
- ²⁸R.R. dos Santos and L. Sneddon, Phys. Rev. B **23**, 3541 (1981).
- ²⁹J. Luo and N.E. Bickers, Phys. Rev. B **48**, 15 983 (1993).